The Journal of Experimental Biology 199, 2703–2712 (1996)
Printed in Great Britain © The Company of Biologists Limited 1996
JEB0522

CONTRACTION DYNAMICS AND POWER PRODUCTION OF PINK MUSCLE OF THE SCUP (*STENOTOMUS CHRYSOPS*)

DAVID J. COUGHLIN*, GUIXIN ZHANG AND LAWRENCE C. ROME†

University of Pennsylvania, Department of Biology, Leidy Laboratory, Philadelphia, PA 19104, USA and *Marine Biological Laboratory, Woods Hole, MA 02543, USA*

Accepted 8 August 1996

Summary

Although the contribution of red muscle to sustained swimming in fish has been studied in detail in recent years, the role of pink myotomal muscle has not received attention. Pink myotomal muscle in the scup (*Stenotomus chrysops*) lies just medial to red muscle, has the same longitudinal fibre orientation and is recruited along with the red muscle during steady sustainable swimming. However, pink muscle has significantly faster rates of relaxation, and the maximum velocity of shortening of pink muscle (7.26±0.18 muscle lengths s^{-1}, *N*=9, at 20 °C, and 4.46±0.15 muscle lengths s^{-1}, *N*=6, at 10 °C; mean ± S.E.M.) is significantly faster than that of red muscle. These properties facilitate higher mass-specific maximum oscillatory power production relative to that of red muscle at frequencies similar to the tailbeat frequency at maximum sustained swimming speeds in scup. Additionally, pink muscle is found in anatomical positions in which red muscle produces very little power during swimming: the anterior region of the fish, which undergoes the lowest strain during swimming. Pink muscle produces more oscillatory power than red muscle under low-strain conditions (±2–3 %) and this may allow pink muscle to supplement the relatively low power generated by red muscle in the anterior regions of swimming scup.

Key words: scup, *Stenotomus chrysops*, pink muscle, muscle mechanics, work production, power.

Introduction

The anatomical separation of different myotomal muscle fibre types of fish has made them an important experimental model for understanding how muscle fibre types differ in their contraction properties and usage during locomotion. Muscle mechanics experiments have shown that red muscle has a relatively low maximum velocity of shortening (V_{max}) and slow activation–relaxation kinetics, while white muscle has a high V_{max} and fast activation–relaxation kinetics (Rome *et al.* 1988; Altringham and Johnston, 1990; Curtin and Woledge, 1988). Accordingly, electromyographic (EMG) evidence has shown that red fibres are used at slow swimming speeds (low shortening velocities and low tailbeat frequencies), whereas white fibres are used at high swimming speeds and during the escape response (high shortening velocities and high tailbeat frequencies) (Bone, 1966; Johnston *et al.* 1977; Rome *et al.* 1984, 1985, 1988, 1992).

By contrast, very little is known about the contractile properties and use of the third myotomal fibre type – pink muscle. Pink muscle lies in a thin sheet between the superficial red muscle and the deeper white muscle. Because of its relative inaccessibility and the difficulty in distinguishing it from red muscle during dissection, no mechanical measurements have been made on myotomal pink muscle.

Myotomal pink muscle is assumed to have contractile properties intermediate between those of red and white muscle. This assumption is based, in part, on isometric relaxation rates observed experimentally in jaw muscles (Akster *et al.* 1985; Akster, 1985) and biochemical assays of myofibrillar ATPase of myotomal muscle showing intermediate values for pink relative to red and white muscle (Johnston *et al.* 1977). In addition, Johnston *et al.* (1977) have shown that pink muscle is recruited at intermediate swimming speeds relative to red and white muscle.

These data suggest that pink muscle may play a crucial role during sustainable swimming. Pink muscle, with its predicted faster rates of relaxation and activation, may be particularly important to power production in regions of the fish in which red muscle produces little power (Rome *et al.* 1993). In scup *Stenotomus chrysops*, the posterior red muscle undergoes relatively high strains during swimming and produces high levels of mass-specific power, while the anterior muscle undergoes relatively low strains and produces much less mass-specific power (Rome *et al.* 1993). The relatively slow

*Present address: Science Division, Widener University, 1 University Place, Chester, PA 19013, USA.
†Author for correspondence (e-mail: lrome@mail.sas.upenn.edu).

relaxation rate of red muscle contributes to the lower power production associated with low strain during oscillatory activity. The predicted faster contraction kinetics of pink muscle may thus permit it to contribute to power production in anterior regions of the fish. Further, the role of pink muscle may be particularly important at low temperatures where relaxation rate is very slow in red muscle (Rome and Swank, 1992).

A three-dimensional map of fibre types in scup has recently been developed in this laboratory (Zhang *et al.* 1996), and regions which contain high proportions of pink fibres have been identified. This facilitates the dissection of bundles of pink muscle fibres from the scup myotome. In the present paper, we compare pink muscle contraction kinetics and power production with those of red muscle in scup. We first characterized force production, activation and relaxation rates, and the maximum velocity of shortening of pink muscle. We then measured mass-specific power production by pink muscle under optimized work-loop conditions (stimulation and length conditions that maximize power) to permit predictions of the swimming speeds over which pink muscle could contribute to power generation. Lastly, to assess the power production of pink muscle during locomotion, we examined mass-specific power production by pink muscle under *in vivo* activity patterns of red muscle (i.e. muscle length change, EMG duration and phase) in swimming fish. No data are available on the activity patterns of pink muscle in swimming scup, so red muscle conditions were used as a first level of inquiry.

Materials and methods

Preparation

Scup (*Stenotomus chrysops*, L.) were collected along the shore of Cape Cod, Massachusetts, USA. The fish, which had a mean (± S.D.) body length of 22.7±2.1 cm (N=22), were killed by a blow to the head and transection of the spinal cord. The scales were removed and strips of muscle 0.9 mm wide were dissected from the region at 35–50 % of the total length behind the snout. This region corresponds to the ANT-2 region used by Rome *et al.* (1993), and the pink layer in this region was determined histochemically to be more than 90 % pink fibres (Fig. 1). Subsequent dissection was carried out at 4 °C with the use of a stereomicroscope. Dissection and experiments were carried out in a physiological saline solution containing (in mmol l^{-1}) 132 NaCl, 2.6 KCl, 2.7 $CaCl_2$, 10 imidazole, 10 pyruvate and 1 $MgCl_2$, pH buffered to 7.7 at 15 °C (based on Altringham and Johnston, 1990). The skin and red muscle layer were removed from the strip of muscle, and a single bundle the length of one myomere (4–6 mm) and with an approximate cross-sectional area of 0.5 mm^2 was isolated. The bundle was tied to a servomotor arm and to a force transducer.

Experimental apparatus and design

Muscle length changes were applied using a Cambridge Technology 300S servosystem, and force was measured with a Cambridge Technology 400 force transducer (natural frequency 2 kHz). All experiments were controlled using a computer *via* an Analog Devices RT-815 D/A board. The muscle bundle was stimulated through platinum plate electrodes running the length of the bundle on both sides. Pulse trains for stimulation were produced with a computer-triggered FHC Pulsar 6b stimulator driving a power amplifier. Stimulus patterns, force and muscle length were recorded on a Data Precision model 6000 digital oscilloscope and stored on disk. Subsequent processing of data was on computer. Custom-developed software was used for all experimental procedures.

A series of experimental procedures was carried out on each muscle bundle, although not all measurements were made on all muscle bundles. For each bundle, the stimulus conditions producing maximum tetanic force were determined at 20 °C (pulse duration, 0.5–1.0 ms; stimulus frequency, 200–400 Hz; stimulus duration, 100–150 ms). When a bundle was also examined at 10 °C, the stimulation conditions were again optimized for maximum tetanic force at that temperature (pulse duration, 1.2–2.0 ms; stimulus frequency, 100–200 Hz; stimulus duration, 200–250 ms). A force–length curve was determined at 20 °C. The length of the muscle bundle was then set such that a 5 % increase or decrease in muscle length would generate approximately the same drop in tetanic force. The average muscle fibre length was measured with a dissecting microscope. The resting tension at this muscle length ranged from 2.4 to 10 % [5.82±2.79 % (S.E.M.)] of maximum tetanic force, but work loop experiments were not performed on bundles with resting tension greater than 5 %. Maximal twitch and tetanus force values were then measured at 10 and 20 °C.

For some preparations, V_{max} was measured at 10 °C and/or 20 °C by using the force-clamp method to construct the force–velocity curve. Shortening velocity was measured at loads between 0.05 and 0.8P_0, where P_0 is the maximum tetanic force. As in most muscles, velocity slows as shortening progresses (Rome and Sosnicki, 1990). Hence, initial velocity was estimated as follows: at low loads, length changes were measured over a 5 ms period starting approximately 7 ms after the release. At higher loads, length changes were measured over a longer period (up to 30 ms) to permit a significant length change. Measurements in this case started approximately 10 ms following release. V_{max} was found by fitting a Hill equation hyperbola to the force–velocity data, after correcting for passive tension (Rome and Sosnicki, 1990; Rome *et al.* 1992). The fit of the hyperbolic curves was improved by not constraining the curves to pass through an intercept of P_0=1 (Rome and Sosnicki, 1990). Steady-state power production during shortening was calculated as the product of force and velocity (see Fig. 5).

Oscillatory power production was studied by stimulating the muscle while imposing a length-change cycle (Josephson, 1985). This was repeated over the selected group of oscillation frequencies. A triangular (ramp) waveform was used for the length oscillations, which approximates the shape of the muscle length-change waveform in the red muscle of swimming scup. Peak values of the waveform were smoothed

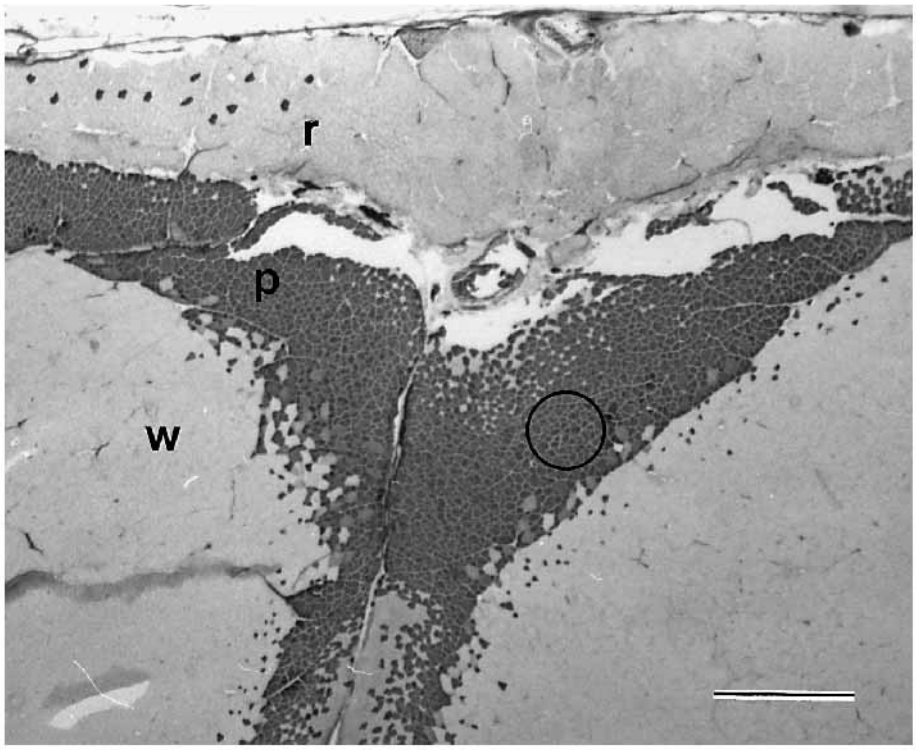

Fig. 1. Cross section of scup myotomal muscle at the ANT-2 position stained with myosin ATPase (alkali pre-incubation, pH 10.2). Pink fibres (p) are stained dark, unstained small fibres are red muscle fibres (r) and unstained large fibres are white muscle fibres (w). The lateral margin of the fish is at the top, and dorsal is to the left. Scale bar, 1.0 mm. The circle represents the region from which muscle bundles of relatively pure pink-fibre content were dissected.

to avoid abrupt changes in muscle direction (as in Rome *et al.* 1993). At 20 °C, the oscillation frequencies were 2, 3, 4, 5, 6, 7.5, 10 and 15 Hz, while at 10 °C they were 2, 2.5, 3, 3.5, 4, 5 and 7.5 Hz. The net work per oscillation cycle was calculated as the difference between positive work (the product of force and length change during the shortening phase of the cycle) and negative work (the product of force and length change during the lengthening phase of the cycle). Oscillatory power was calculated as the product of the net work per cycle and the frequency of oscillation. For each frequency at each temperature, the stimulus and length-change conditions under which muscle bundles generated maximum power were determined; they included the optimal amplitude of the length change, the optimal stimulus duration and the optimal stimulus phase. Stimulus phase, which is usually negative, is defined as the time of onset of the stimulus train with respect to the time of peak muscle length (onset of shortening).

Power production by pink muscle bundles was subsequently measured when the muscle was driven with the *in vivo* muscle activity patterns (including length change, EMG duration and phase) measured for red muscle at 10 and 20 °C for several swimming speeds (Rome *et al.* 1993; L. C. Rome and D. Swank, in preparation). These swimming speeds at each temperature included the maximum speed before recruitment of white muscle (80 cm s^{-1} or approximately 4 body lengths s^{-1} at 20 °C, and 50 cm s^{-1} or approximately 2.5 body lengths s^{-1} at 10 °C).

Histological analysis

After each experiment, the muscle bundle was stained with Trypan Blue to identify dead tissue (Sosnicki *et al.* 1989), embedded in gelatin, frozen in liquid nitrogen, sectioned at 12 µm and separately stained with either succinic dehydrogenase (SDH) for mitochondrial content or myosin ATPase with an alkaline pre-incubation (pH 10.2) to stain pink muscle fibres (Zhang *et al.* 1996). The cross section of live muscle fibres within the bundle and the proportion of the live cross section composed of pink fibres could then be determined. In general, only a few dead fibres (damaged during dissection) were found on the periphery on the muscle bundle. Red and pink fibres could be distinguished on the basis of their different staining patterns (Zhang *et al.* 1996). Pink fibres stained darkly with myosin ATPase, but lightly with SDH. Red fibres were not stained by myosin ATPase but were darkly stained by SDH. Fibres unstained by either technique were white muscle fibres. All results are presented as mean ± S.E.M. unless otherwise noted.

Results

Isometric contractions

All of the experimental muscle bundles were taken from the ANT-2 position of scup. The cross-sectional areas of the muscle bundles were 93.8±7.0 % (± S.D., N=22) pink fibres, with the remainder of live muscle being red fibres (Fig. 1). Maximum tetanic forces were 151.0±8.9 kN m^{-2} at 20 °C and 122.8±12.7 kN m^{-2} at 10 °C (Q_{10}=1.17). Maximum twitch forces were 62.2±5.5 kN m^{-2} at 20 °C and 63.4±5.3 kN m^{-2} at 10 °C (Q_{10}=0.90). The twitch/tetanus ratio at 20 °C was 0.417±0.032 and that at 10 °C was 0.532±0.093.

Pink muscle fibres showed faster activation and relaxation rates relative to red muscle fibres (Fig. 2). Temperature had a

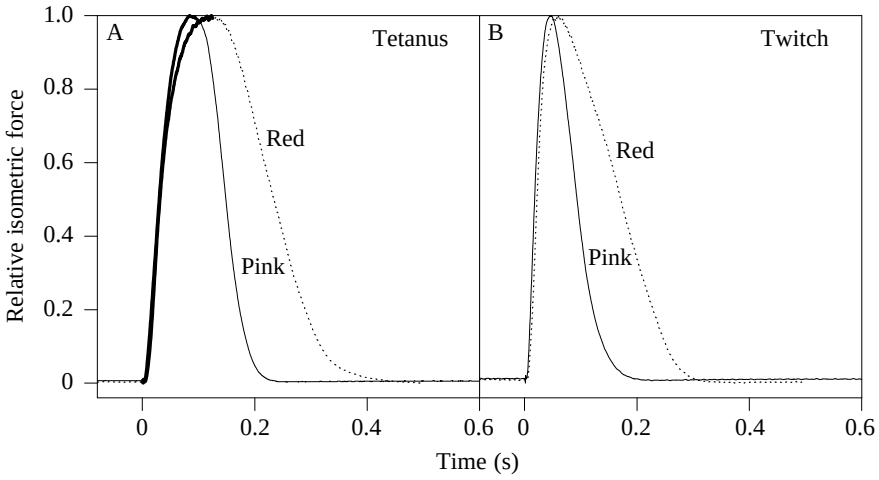

Fig. 2. Tetanus (A) and twitch (B) records at 20 °C for red and pink muscle bundles. Individual traces were normalized to the peak force of that contraction. For each record, the stimulus (either a repeated train of pulses for tetanus or a single pulse for twitch stimulation) was optimized such that the muscle bundle generated maximum force. Stimulation began at time zero. The stimulation duration of the tetanus (A) is represented by the thickening of the force trace. Because pink muscle does not maintain steady tetanic force for as long as red muscle, tetanus stimulation duration was limited and the broad plateau observed for the red muscle tetanus record was not observed in pink muscle tetanus records.

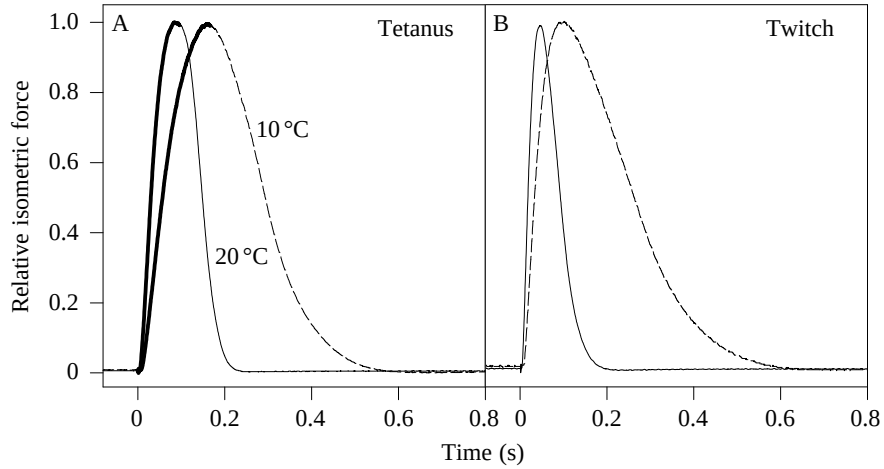

Fig. 3. Tetanus (A) and twitch (B) records at 10 °C and 20 °C for a pink muscle bundle. Individual traces were normalized to the peak force of that contraction. Stimulation conditions are as in Fig. 2.

large effect on relaxation rates of pink muscle, with Q_{10} values for twitch and tetanus relaxation rates ranging from 2.41 to 3.54 (Fig. 3; Table 1). Activation rates were less temperature-sensitive, having a Q_{10} of approximately 2 for both twitch and tetanus (Table 1).

Velocity of shortening

V_{max} of pink muscle was 7.26±0.18 muscle lengths s^{-1} at 20 °C (N=9) and 4.46±0.15 muscle lengths s^{-1} at 10 °C (N=6; Q_{10}=1.6; Figs 4, 5; Table 2). At 20 °C, the maximum steady-state power was generated at a V/V_{max} of 0.31±0.05; at 10 °C, it was generated at a V/V_{max} of 0.32±0.05. The Hill constant of the force–velocity curves, a/P_0*, was 0.29±0.06 at 20 °C and 0.37±0.09 at 10 °C, where P_0* is the intercept of the curve on the force axis.

Oscillatory work production

During oscillatory activity (work loops), the maximum oscillatory power produced by pink muscle at 20 °C was 43.6±4.2 W kg^{-1} wet muscle mass (N=15) and occurred at an

Table 1. *Activation and relaxation times for twitches and tetani of pink muscle bundles*

	$T_{a\ 10–90}$ (ms)	$T_{r\ 90–10}$ (ms)	$T_{r\ 95–80}$ (ms)	$T_{r\ last}$ (ms)
Twitch				
20 °C	22.7±3.5	73.5±18.2	14.2±4.1	135.0±27.5
10 °C	45.1±8.1	260.7±58.8	40.5±12.6	396.2±80.1
Q_{10}	2.02	3.54	2.86	2.94
Tetanus				
20 °C	44.5±11.5	82.2±19.3	19.4±5.7	109.3±23.5
10 °C	83.6±13.5	233.0±49.9	46.8±16.5	318.1±64.6
Q_{10}	1.87	2.83	2.41	2.91

Values are means ± S.E.M. (N=12 for all).

Activation time from 10 to 90 % of maximum force ($T_{a\ 10–90}$) and relaxation times from 90 to 10 % of maximum force ($T_{r\ 90–10}$), from 95 to 80 % of maximum force ($T_{r\ 95–80}$) and from the end of the stimulus to 10 % of maximum force ($T_{r\ last}$) are given.

Q_{10} values are for the inverse of activation and relaxation times (i.e. activation and relaxation rates).

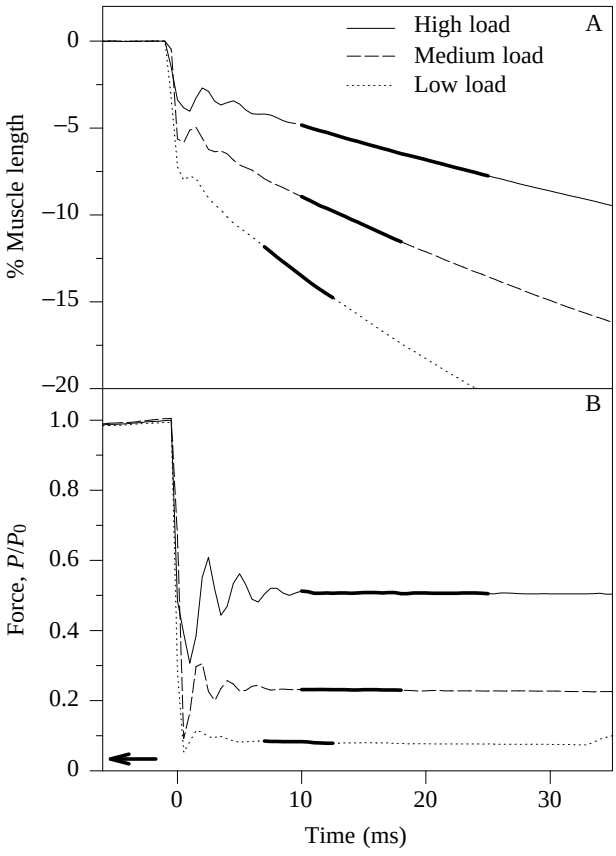

Fig. 4. Force clamp traces from a pink muscle bundle. Length (A) and force (B) records are shown for three force clamps at high, medium and low loads. The bundle was released 100 ms into the contraction after steady isometric force had been reached. The bold segment of the traces signifies the measurement period. The resting tension at the initial muscle length (3.75 mm) is shown by the horizontal arrow. Resting tension was 3 % of maximum isometric tension (P_0). Note that, at the length where velocity was measured for the lightest load shown, the passive tension was only approximately 30 % of the resting tension.

optimal cycle frequency (F_{opt}) of 6–7.5 Hz (Table 2; Figs 6, 7A). The largest power value was obtained after 5–6 cycles, when power production had levelled off to a constant value for several cycles. At 10 °C, maximum oscillatory power production was 14.2±1.0 W kg^{-1} (N=10) and was found at an F_{opt} of 3.0–4.0 Hz (Table 2; Figs 6, 7B). The Q_{10} for maximum oscillatory power production was 3.07. The Q_{10} for maximum oscillatory power at a given frequency increased with oscillation frequency from 0.94 at 2 Hz to 5.2 at 7.5 Hz.

The stimulation conditions under which muscle bundles generated the highest oscillatory power at a given frequency varied with frequency (Fig. 8). Stimulus phase became more negative (i.e. the stimulus preceded the shortening portion of the length change by a greater percentage of the cycle) and peak strain decreased with increasing frequency at both 10 °C and 20 °C. The absolute duration of the stimulus decreased with increasing frequency. However, the stimulus duty cycle (stimulus duration relative to oscillation period) first increased and then decreased with increasing frequency.

Power production and in vivo *activity patterns*

The activity patterns of red muscle in swimming fish (termed the *in vivo* muscle activity pattern, which include oscillation frequency, strain, and stimulus duration and phase) have been measured previously at a variety of swimming speeds, body positions and temperatures for scup (Rome *et al.* 1993; L. C. Rome and D. Swank, in preparation). Four muscle positions ranging from 29 to 70 % of the total length from the snout were used and were termed ANT-1, ANT-2, MID and POST

Table 2. *Comparison of contraction properties and power production of pink and red muscle at 10 and 20 °C*

	10 °C		20 °C	
	Red muscle	Pink muscle	Red muscle	Pink muscle
$T_{a\ 10–90}$ (ms)	127.3±22.2 (5)	90.7±13.5 (12)	57.6±1.68 (5)	44.5±11.5 (12)
$T_{r\ 90–10}$ (ms)	685.2±118.8 (5)	247±49.9 (12)*	165±18.7 (5)	82.5±19.3 (12)*
V_{max} (muscle lengths s^{-1})	3.32±0.16 (8)	4.46±0.15 (6)*	5.55±0.25 (8)	7.26±0.18 (9)*
Steady-state $\dot{W}_{max}$ (W kg^{-1})	70.9±8.1 (8)	67.7±6.9 (6)	134±13 (8)	133±19.0 (9)
F_{opt} (Hz)	2.5	3.0–4.0	5.0	6.0–7.5
Oscillatory $\dot{W}_{max}$ (W kg^{-1})	12.8±2.1 (6)	14.2±1.0 (10)	27.6±1.2 (6)	43.6±4.2 (15)*

Values are mean ± S.E.M. (N).

All muscle bundles are from the ANT-2 position of scup.

Activation time from 10 to 90 % of maximum force ($T_{a\ 10–90}$) and relaxation times from 90 to 10 % of maximum force ($T_{r\ 90–10}$) are given. Activation and relaxation times are for tetanus.

Determination of maximum velocity of shortening (V_{max} in muscle lengths s^{-1}), maximum steady-state power production (steady-state, $\dot{W}_{max}$, in W kg^{-1}) and the optimal frequency of oscillation (F_{opt} in Hz) is described in the text.

Maximum oscillatory power production (oscillatory, $\dot{W}_{max}$, in W kg^{-1}) is from optimized work loops.

Data on red muscle are from the following sources: V_{max} (Rome *et al.* 1992); activation and relaxation rates and power production at 20 °C (Rome *et al.* 1993); activation and relaxation rates and power production at 10 °C and activation rates (L. C. Rome, unpublished data); optimal frequency of oscillation (Rome and Swank, 1992).

An asterisk indicates a significant difference between red and pink muscle for a particular characteristic and temperature (t-test, P<0.05).

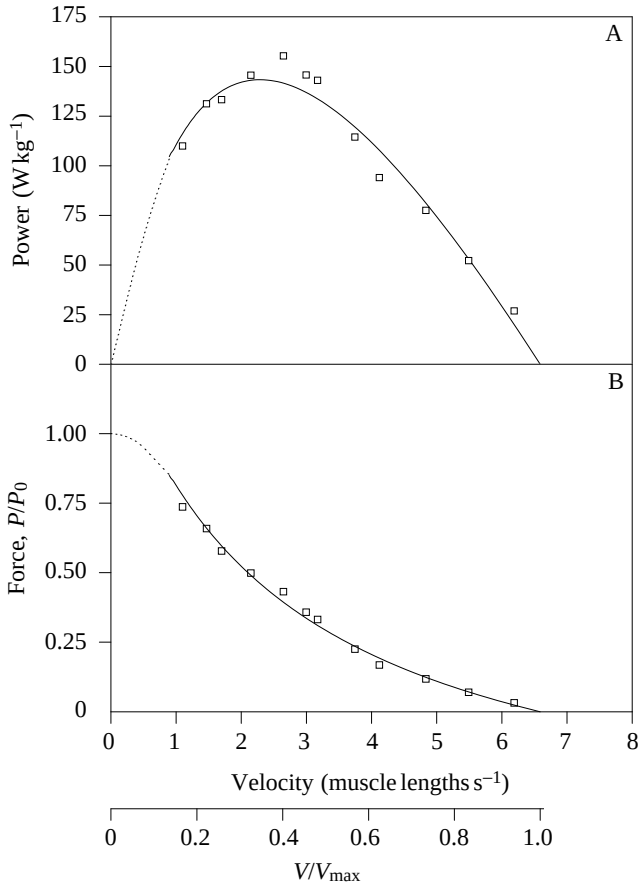

Fig. 5. Power–velocity (A) and force–velocity (B) curves for a pink muscle bundle at 20 °C. Raw data from a single pink muscle bundle are shown. A Hill equation hyperbola was fitted to the data in B as described in the text. Above loads of $0.8P_0$, the curve is approximated by a spline fit. Steady-state power, the product of force and velocity, is plotted in A. The V_{max} of the bundle shown is 6.59 muscle lengths s^{-1}.

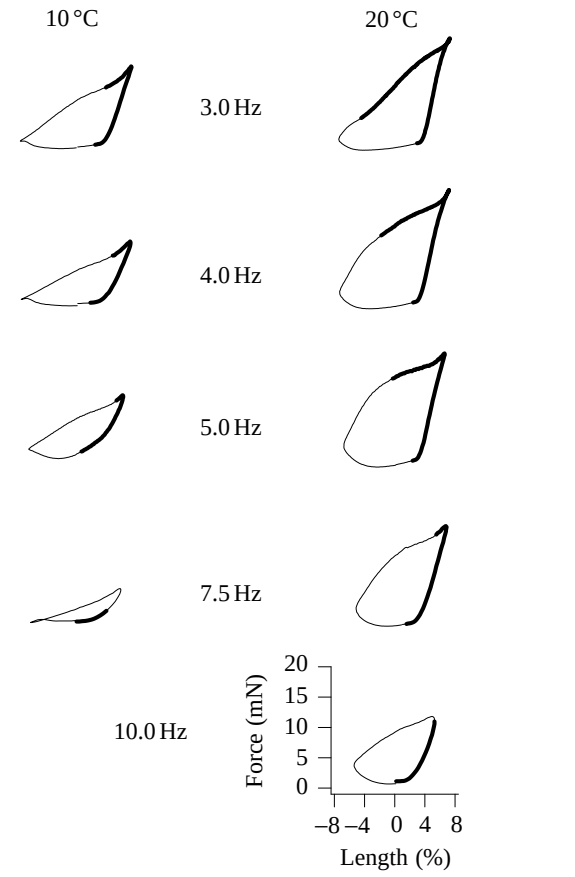

Fig. 6. Optimized work loops for oscillatory activity by pink muscle at 10 °C and 20 °C. Individual work loops are presented as a plot of force (mN) *versus* muscle length change from resting length (mm). The area of the loop is a measure of the net work generated during one oscillation (work = force × length change). The thickening of the trace indicates the period of stimulation.

respectively (Rome *et al.* 1993). For this study, the *in vivo* activity patterns recorded from the four positions in fish swimming at their maximum sustainable speeds (powered by red and pink muscle only) at 10 °C and 20 °C were used (50 cm s^{-1} and 4.0 Hz tailbeat frequency at 10 °C, and 80 cm s^{-1} and 6.4 Hz at 20 °C).

When stimulated under these *in vivo* conditions, at 20 °C, pink muscle (dissected from the ANT-2 position 40 % of total length behind the snout) generated positive work for the conditions from all muscle positions. At 10 °C, power production under the ANT-1 conditions did not differ significantly from zero (*t*-test, $P>0.05$), while the three more posterior positions produced positive power (Table 3).

Table 3. *Oscillatory power production of pink and red muscle bundles under* in vivo *activation patterns of red muscle in swimming scup*

	Red muscle 20 °C	Pink muscle 20 °C	Pink/red 20 °C	Pink muscle 10 °C
ANT-1	4.4±0.8	12.4±1.7	2.82*	0.3±0.7
ANT-2	6.6±0.6	29.1±1.9	4.40*	1.3±0.6
MID	10.8±0.6	38.6±2.2	3.57*	6.8±0.7
POST	24.32±4.3	38.4±4.8	1.58	11.3±0.4

Values of power production (W kg^{-1}) are mean ± S.E.M.; N=4 at 10 and 20 °C for pink muscle; N=6 at 20 °C for red muscle.

The *in vivo* conditions are those that occur during swimming at the approximate maximum sustained swimming speed which corresponds to 0.80 m s^{-1} and a tailbeat frequency of 6.4 Hz at 20 °C and 0.50 m s^{-1}, and a tailbeat frequency of 4.0 Hz at 10 °C.

The four positions, ANT-1, ANT-2, MID and POST, represent positions 29, 40, 54 and 70 % of the total length behind the snout.

An asterisk indicates a significant difference between power values for red and pink muscle at 20 °C (*t*-test, $P<0.05$).

The red muscle data are taken from Rome *et al.* (1993).

Discussion

Comparison of the morphology, biochemistry and mechanics of pink and red muscle

The three muscle fibre types found in fishes are named by

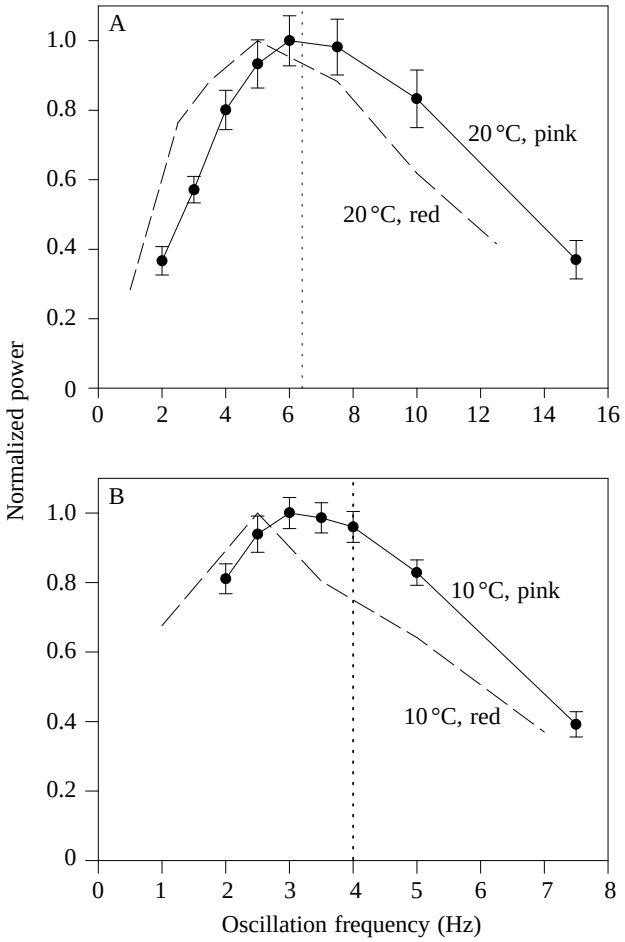

Fig. 7. Power *versus* oscillation frequency for pink muscle at 20 °C (A, *N*=5) and 10 °C (B, *N*=6). Mean maximum oscillatory power production by pink muscle (± S.E.M.) is plotted *versus* oscillation frequency. The corresponding curves for red muscle are also included. For each curve, the power values are normalized for maximum power production. Data for red muscle are from Rome and Swank (1992). Vertical dashed lines represent the tailbeat frequency at the fastest swimming speed prior to white muscle recruitment at each temperature (6.4 Hz at 20 °C and 4.0 Hz at 10 °C; Rome *et al.* 1993).

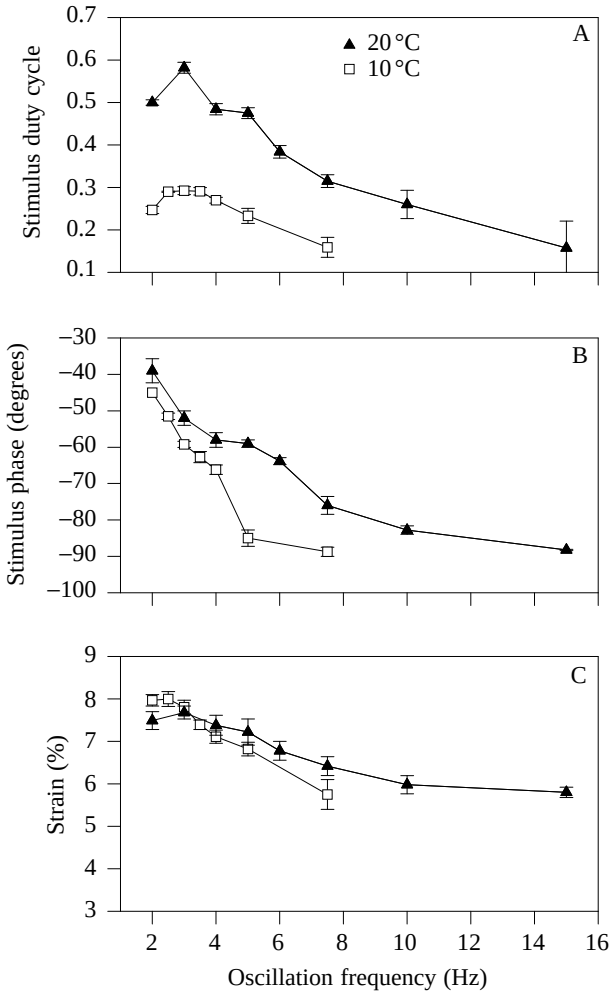

Fig. 8. Optimized stimulus conditions and length change under which pink muscle bundles produced maximum oscillatory power *versus* oscillation frequency for two temperatures, 10 °C and 20 °C: stimulus duty cycle (A), stimulus phase (B) and strain (% muscle length change, C).

their colour: red, pink and white. Their colour is indicative of the level of circulation each muscle type receives. These muscle types are identified on the basis of histochemical staining with myosin ATPase (Mascarello *et al.* 1986) and immunocytochemistry of myosin isoforms. The heavy- and light-chain myosin isoforms of red muscle are different from those of white and pink muscle (Scapolo and Rowlerson, 1987). Also, although pink and white muscle share the same forms of myosin light chain, they have distinct forms of heavy-chain myosin (Scapolo and Rowlerson, 1987).

Only red and pink fibres are active during steady sustainable swimming (carp, Rome *et al.* 1984, Rome *et al.* 1990; scup, Rome *et al.* 1992), whereas white fibres are not (i.e. their use leads to rapid fatigue). Thus, it is useful to compare the properties of red and pink fibres. Pink muscle appears to be intermediate between red and white muscle with regard to several characteristics. Pink muscle has intermediate levels of (1) oxidative and glycolytic enzymatic activities, with higher oxidative activity levels found in red muscle and higher glycolytic activity levels found in white muscle (Patterson *et al.* 1975; Johnston *et al.* 1977; Mascarello *et al.* 1986); (2) myofibrillar ATPase activity, with a reported red:pink:white ratio of 1:2:4 (Johnston *et al.* 1977); and (3) mitochondrial content, with red having the highest and white having the lowest mitochondria volume (Johnston, 1981).

Despite these morphological and biochemical differences, the force generated per unit fibre cross-sectional area is about the same for red and pink fibres. In scup at 20 °C, tetanic force in pink muscle (151±9 kN m^{-2}, *N*=22) is not statistically different (*t*=1.58, *P*=0.13) from that in red muscle (197±20 kN m^{-2}, *N*=9; Rome and Swank, 1992). Similar results have been obtained for the jaw muscles of carp (Granzier *et al.* 1983).

There are, however, large differences in the kinetics of

contraction. The activation and relaxation rates of pink myotomal muscle in scup are faster than those of red muscle. This relationship has been previously shown in carp and perch jaw muscle (Granzier *et al.* 1982, 1983; Akster, 1985; Akster *et al.* 1985). V_{max} in scup at 20 °C for pink muscle (7.26 muscle lengths s^{-1}) is also significantly faster (t=5.64, P<0.001) than that for red muscle (5.55 muscle lengths s^{-1}; Rome *et al.* 1992).

F_{opt} *and tailbeat frequency*

The differences in V_{max} and in activation and relaxation kinetics between red and pink muscle of scup affect mass-specific power production by the two fibre types. Pink muscle produces more oscillatory power than red muscle (t-test, P=0.029; Table 2) and this occurs at a higher F_{opt} than red muscle (Table 2). At 20 °C, the broad plateau of the pink muscle power *versus* frequency curve had an F_{opt} of 6.0–7.5 Hz (centred at 6.75 Hz), approximately 30 % higher than that of red muscle. This increase is approximately the same as the relative increase in V_{max} from red to pink muscle. A 30 % increase from red to pink muscle in both F_{opt} and V_{max} was also observed at 10 °C.

At 20 °C, the F_{opt} of pink muscle (6.75 Hz) corresponds closely to the tailbeat frequency of maximum sustained swimming (6.4 Hz; Rome *et al.* 1993). However, F_{opt} for red muscle at this temperature (5.0 Hz) is considerably below the maximum sustained tailbeat frequency (Fig. 7A). The same relationship is found at 10 °C, where the maximum sustained tailbeat frequency (4.0 Hz) is close to the F_{opt} of pink muscle (3.5 Hz) and considerably higher than the F_{opt} of red muscle (2.5 Hz) (Table 2; Fig. 7B).

Pink and red power and in vivo *activation patterns*

The close match between F_{opt} in pink muscle and the tailbeat frequency of swimming at the maximum sustained speed indicates that pink muscle should produce more mass-specific power than red muscle in fish swimming at that tailbeat frequency. Indeed, when oscillatory power is measured for muscle bundles activated using the *in vivo* activation and length-change patterns observed in red muscle at 20 °C, pink muscle produces significantly more power than red muscle for the ANT-1, ANT-2 and MID positions, with ratios of mass-specific pink to red muscle power production ranging from 3 to 4 for these positions (Table 3). For the muscle-activation and length-change patterns of red muscle at the POST position, there was no significant difference in mass-specific power production of pink and red muscle.

Since pink muscle has the potential to produce more oscillatory power than red muscle under *in vivo* activation and length-change patterns, why does the fish use red muscle at all? An examination of the power *versus* frequency curve for maximized work loops at 20 °C (Fig. 7A) shows that, at lower frequencies (2–3 Hz), red muscle produces more power than pink muscle. This result can be attributed, in part, to a drop in force in pink muscle when operating at lower frequencies. Both pink and red muscle show a reduction of force during the shortening phase of the length-change cycle. However, at low frequencies, the drop in force level in pink muscle is far more dramatic than that observed in red muscle. At higher frequencies (same strain but shorter stimulation duration), pink muscle maintains high force levels during the shortening phase (e.g. 5 Hz at 20 °C, Fig. 6). This suggests that the greater reduction in force in pink muscle than in red muscle at low frequencies is not specifically due to a greater shortening-induced deactivation (as occurs commonly in fish muscle). Rather, it may reflect reduced endurance. The implication of this reduction in force during low-frequency oscillation in pink muscle is that, at lower frequencies of oscillation and when the strain is sufficiently large (5–7 % per cycle), red muscle can produce as much or more mass-specific power than pink muscle (Fig. 7).

Whether the drop in force observed in pink muscle is an experimental artefact or whether it actually occurs in pink muscle during swimming is unknown. Future research will address this issue.

Power production of pink muscle and its morphological distribution

The main advantage of pink muscle over red muscle may be its faster relaxation rate. Shortening deactivation is reduced when the strain is low and, hence, intrinsic relaxation rates can then limit power production under conditions of low strain and moderate-to-high oscillation frequencies. Since pink muscle has a faster intrinsic relaxation rate than does red muscle, it should produce more mass-specific power than red muscle under conditions in which relaxation rate is a limiting factor. At moderate and high oscillation frequencies and low strain, red muscle does not adequately relax prior to the lengthening phase of the length-change cycle and considerable negative work is 'produced' during lengthening. Pink muscle, with faster intrinsic rates of relaxation, will drop to a much lower force level during lengthening than red muscle and therefore much less negative work will be generated.

The greatest differences in power production between red and pink muscle operating under the activation and length-change patterns observed in the red muscle of swimming fish are for the conditions corresponding to the more anterior regions of the fish, where strain is lowest (Rome *et al.* 1992, 1993). Rome *et al.* (1993) reported intrinsic differences in rates of relaxation in red muscle along the length of scup. Muscle from anterior regions of the fish had faster rates of relaxation. As the slower-relaxing red muscle from the POST position produced negative power when activated under the *in vivo* patterns of the ANT-1 muscle, the faster relaxation rates observed in ANT-1 and ANT-2 red muscle appear to be critical to power production in anterior regions of the fish (Rome *et al.* 1993). Since pink muscle has even faster relaxation rates than the fastest red muscle, it follows that it should produce more power than red muscle. The faster relaxation rate of pink muscle will have the greatest effect on power production during swimming in areas of low strain – the anterior regions of the fish.

The region in which pink muscle would make the greatest contribution to power production during swimming is also the region in which the most pink swimming muscle is found in scup. While approximately twice as much red muscle is found in the posterior region of the fish as in the anterior region, pink muscle has an approximately twofold greater cross section in the anterior regions than the posterior regions (Zhang *et al.* 1996). Thus, whereas the pink muscle volume is only approximately 17 % of the red muscle volume in the POST position of the fish, in the ANT-1 position, it is approximately 75 %. At the ANT-1 and ANT-2 positions, there is a region of pink muscle with relatively pure pink fibre composition; at the POST position, there is no pink layer. Rather, at the POST position, just a few pink fibres are mixed with red muscle fibres at the medial margin of the red muscle layer. The MID region shows a condition intermediate between ANT-2 and POST: a nearly even mixture of pink and red muscle fibres in a layer lying medial to the larger red muscle layer (Zhang *et al.* 1996). Thus, at the locations where mass-specific power production by red muscle is significantly reduced by low strain during swimming and where the quantity of red muscle is lowest, there is the greatest concentration of the pink fibres that are capable of producing significant mass-specific power at low strain.

Although they have the same fibre orientation (parallel to the long axis), pink and red muscle are found at different depths. Because pink muscle lies closer to the backbone, it will undergo lower strain during swimming than the overlying red muscle. On the basis of their relative depth, the ratio of pink muscle strain to red muscle strain is estimated to be 82 % at the MID, 87 % at the ANT-2 and 91 % at the ANT-1 positions. Thus, the 3.0 % strain observed in red muscle at the ANT-2 position of a scup swimming at 80 cm s^{-1} would correspond to a strain of 2.6 % for the underlying pink muscle. This lower strain increases the need for faster relaxation rates to permit positive power production. If power production is limited in red muscle because of the low strain of the anterior regions of the fish, faster-relaxing muscle is necessary to generate power at deeper depths, where strain is even lower. In addition, the limitations of red muscle will be exacerbated at lower temperatures. At 10 °C, relaxation rates are much slower (Rome and Swank, 1992) and power production by red muscle drops even further for conditions of low strain during swimming (L. C. Rome, unpublished data). Since scup experience such cold water temperatures in the winter (down to approximately 7 °C in the Gulf Stream; Neville and Talbot, 1964), pink muscle may contribute substantially to power production for swimming at low temperatures.

In summary, the faster rates of relaxation and activation and the faster maximum shortening velocity of scup pink muscle facilitate higher maximum power production relative to red muscle at oscillation frequencies similar to the maximum sustained swimming speeds. Additionally, pink muscle is relatively abundant in anatomical positions in which the relaxation properties of red muscle might be inadequate for high mass-specific power production: the ANT-1 and ANT-2 positions that undergo the lowest strain rates during swimming. In more posterior regions of the fish, which undergo high strain during swimming, little pink muscle is found. In the posterior regions, red muscle can produce nearly as much mass-specific power as pink muscle at the oscillation frequencies observed in scup swimming sustainably. The future of this research is to examine the activity of pink muscle during swimming in fish. Characterization of pink muscle activity patterns *in vivo* will permit accurate assessment of power production by pink muscle during swimming.

We thank Douglas Swank, Douglas Syme and Gordon Lutz for technical support and comments on this manuscript. This work was supported by NIH AR38404 and NSF IBN 9514383 to L.C.R. and an NIH postdoctoral fellowship to D.J.C.

References

AKSTER, H. A. (1985). Morphometry of muscle fibre types in the carp (*Cyprinus carpio* L.), relationships between structural and contractile characteristics. *Cell Tissue Res.* **241**, 193–201.

AKSTER, H. A., GRANZIER, H. L. M. AND TER KEURS, H. E. D. J. (1985). A comparison of quantitative ultrastructural and contractile characteristics of muscle fibre types of the perch (*Perca fluviatilis* L.). *J. comp. Physiol.* B **155**, 685–691.

ALTRINGHAM, J. D. AND JOHNSTON, I. A. (1990). Modelling muscle power output in a swimming fish. *J. exp. Biol.* **148**, 395–402.

BONE, Q. (1966). On the function of the two types of myotomal muscle fibres in elasmobranch fish. *J. mar. biol. Ass. U.K.* **46**, 321–349.

CURTIN, N. A. AND WOLEDGE, R. C. (1988). Power output and force–velocity relationship of live fibres from white myotomal muscle of the dogfish, *Scyliorhinus canicula*. *J. exp. Biol.* **140**, 187–197.

GRANZIER, H. L. M., WIERSMA, J., AKSTER, H. A. AND OSSE, J. W. M. (1983). Contractile properties of a white- and a red-fibre type of the m. hyohyoideus of the carp (*Cyprinus carpio* L.). *J. comp. Physiol.* **149**, 441–449.

GRANZIER, H. L. M., WIERSMA, J., OSSE, J. W. M., AKSTER, H. A. AND VAN DOMMELEN, W. M. C. M. (1982). Contractile properties of a white and a red fibre type of the m. hyohyoideus of the carp (*Cyprinus carpio*). *J. Muscle Res. Cell Motil.* **3**, 122.

JOHNSTON, I. A. (1981). Structure and function of fish muscles. *Symp. zool. Soc., Lond.* **48**, 71–113.

JOHNSTON, I. A., DAVISON, W. AND GOLDSPINK, G. (1977). Energy metabolism of carp swimming muscles. *J. comp. Physiol.* **114**, 203–216.

JOSEPHSON, R. K. (1985). Mechanical power output from striated muscle during cyclic contraction. *J. exp. Biol.* **114**, 493–512.

MASCARELLO, F., ROMANELLO, M. G. AND SCAPOLO, P. A. (1986). Histochemical and immunohistochemical profile of pink muscle fibres in some teleosts. *Histochem.* **84**, 251–255.

NEVILLE, W. C. AND TALBOT, G. B. (1964). The fishery for scup with special reference to yield and their causes. *U.S. Dept. Int. U.S. Fish Wildl. Serv., Spec. Sci. Rep. Fish.* **459**, 61pp.

PATTERSON, S., JOHNSTON, I. A. AND GOLDSPINK, G. (1975). A histochemical study of the lateral muscles of five teleost species. *J. Fish Biol.* **7**, 159–166.

ROME, L. C., FUNKE, R. P., ALEXANDER, R. MCN., LUTZ, G., ALDRIDGE, H. D. J. N., SCOTT, F. AND FREADMAN, M. (1988). Why animals have different muscle fibre types. *Nature* **366**, 824–827.

ROME, L. C., FUNKE, R. P. AND ALEXANDER, R. M. (1990). The influence of temperature on muscle velocity and sustained performance in swimming carp. *J. exp. Biol.* **154**, 163–178.

ROME, L. C., LOUGHNA, P. T. AND GOLDSPINK, G. (1984). Muscle fiber recruitment as a function of swim speed and muscle temperature in carp. *Am. J. Physiol.* **247**, R272–R270.

ROME, L. C., LOUGHNA, P. T. AND GOLDSPINK, G. (1985). Temperature acclimation improves sustained swimming performance at low temperatures in carp. *Science* **228**, 194–196.

ROME, L. C. AND SOSNICKI, A. J. (1990). The influence of temperature on mechanics of red muscle in carp. *J. Physiol., Lond.* **427**, 151–169.

ROME, L. C., SOSNICKI, A. J. AND CHOI, I.-N. (1992). The influence of temperature on muscle function in fast swimming scup. II. The mechanics of red muscle. *J. exp. Biol.* **163**, 281–295.

ROME, L. C. AND SWANK, D. (1992). The influence of temperature on power output and scup red muscle during cyclical length changes. *J. exp. Biol.* **171**, 261–281.

ROME, L. C., SWANK, D. AND CORDA, D. (1993). How fish power swimming. *Science* **261**, 340–343.

SCAPOLO, P. A. AND ROWLERSON, A. (1987). Pink lateral muscle in the carp (*Cyprinus carpio* L.): histochemical properties and myosin composition. *Experientia* **43**, 384–386.

SOSNICKI, A. A., LUTZ, G., ROME, L. C. AND GOBLE, D. O. (1989). Histochemical and molecular determination of fiber types in chemically skinned single equine muscle cells. *J. Histochem. Cytochem.* **37**, 1731–1738.

ZHANG, G., SWANK, D. M. AND ROME, L. C. (1996). Quantitative distribution of muscle fiber types in the scup. *J. Morph.* **229**, 71–81.